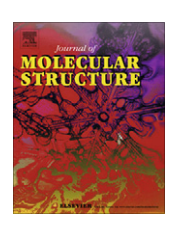
ELSEVIER

Contents lists available at SciVerse ScienceDirect

Journal of Molecular Structure

journal homepage: www.elsevier.com/locate/molstruc



Synthesis of chromium(III) complex with 1-hydroxy-2-pyridinone-6-carboxylic acid as insulin-mimetic agent and its spectroscopic and computational studies

Nuttawisit Yasarawan a, Khajadpai Thipyapong a,*, Somsak Sirichai a, Vithaya Ruangpornvisuti b

HIGHLIGHTS

- ► Chromium complex with 1-hydroxy-2-pyridinone-6-carboxylic acid was synthesized.
- ▶ DFT computations agreed with experimental spectroscopic data.
- ▶ The complex showed insulin mimetic activity.

ARTICLE INFO

Article history: Received 23 March 2012 Received in revised form 20 July 2012 Accepted 23 July 2012 Available online 31 July 2012

Keywords: HOPO Chromium complex 1-Hydroxy-2-pyridinone-6-carboxylic acid DFT TDDFT PCM

ABSTRACT

The new complex of chromium(III) and 1-hydroxy-2-pyridinone-6-carboxylic acid was synthesized and its preparation routes were reported. Mass spectrometry and elemental analysis indicated the formation of chromium complex with the metal-to-ligand mole ratio of 1:3. Combination of spectroscopic measurement and spectral computations based on the density functional theory suggested that 1-hydroxy-2-pyridinone-6-carboxylic acid was a bidentate ligand using one oxygen atom at pyridinone carbonyl group and the other at N-oxide group as donor atoms upon chelation with chromium(III), forming the six-coordinate complex with five-membered chelate rings. Due to the enhanced stability of the chelate rings, such the pathway of chelation was theoretically predicted to be more favorable than the case where the carboxylate oxygen atom of ligand participated in the chelation. According to the preliminary tests, the chromium(III) complex with 1-hydroxy-2-pyridinone-6-carboxylic acid was found to be active in lowering plasma glucose levels in vivo.

© 2012 Elsevier B.V. All rights reserved.

1. Introduction

Development of insulin-mimetic compounds based on metal complexes has been of pharmaceutical interest since a number of particular transition metal ions, for example, chromium(III) [1–3], vanadium(IV) [4–6], and zinc(II) [4,7–11] have been found to significantly decrease blood glucose levels both in vivo and in vitro. Effects of chromium supplementation on humans and animals in many aspects have been well summarized by Anderson [2,3]. Although the mechanisms for the anti-diabetic effects of chromium(III) remain uncertain, it has been proposed that the biologically active form of chromium enhances insulin signaling by promoting insulin receptor tyrosine kinase activity leading to glucose uptake [12,13]. Among other metal complexes, chromium(III) picolinate has successfully become a nutritional supplement used for preventing high blood sugar levels [1,14,15]. However, it has been reported that the picolinate ligand may cause

adverse effects such as morphological defects in offspring of mice [16] or DNA mutations through the formation of hydroxyl radicals in the presence of biological reductants [15,17]. A number of studies have therefore emphasized the importance of using biologically friendly chelating agents, e.g. p-phenylalanine [18-21], N-acetyl-L-cysteine [22], maltol [10,23], ethyl maltol [24], citric acid [25] or flavonoids [26,27] in the preparation of anti-diabetic metal complexes. Interestingly, 1-hydroxy-2-pyridinone (or 1,2-HOPO) and its related compounds form a family of chelating agents which are potential for use either as gadolinium-based magnetic resonance imaging (MRI) contrast agents [28-30] or iron chelator in the therapy of iron-related blood disease [31]. An enterobactin analog known as 1,2-hopobactin may find application in the treatment of iron overload as such the compound was found to form a ferric complex isostructural with the corresponding complex formed by siderophore enterobactin (a microbial iron-chelating agent) [32]. Various types of 1,2-HOPO-based compounds were synthesized with the aim at achieving potential sequestering agents for removing radionuclide contamination in the body by means of in vivo chelation [33-37]. Recently,

^a Department of Chemistry, Faculty of Science, Burapha University, Chonburi 20131, Thailand

^b Department of Chemistry, Faculty of Science, Chulalongkorn University, Bangkok 10330, Thailand

^{*} Corresponding author. Tel.: +66 38 103 069; fax: +66 38 393 494. E-mail address: khajadpa@buu.ac.th (K. Thipyapong).

luminescence properties of the Eu(III) complexes with the ligands containing 1,2-HOPO units have been investigated both experimentally and theoretically [38,39]. Since 2002, the improved method to synthesize a carboxyl derivative of 1,2-HOPO, namely 1,2-HOPO-6-carboxylic acid (or 1-hydroxy-2-pyridinone-6-carboxylic acid), has been established by Xu et al. Such the 1,2-HOPO derivative exhibited high selectivity in binding to Fe(III) and Pu(IV) whose the charge-to-radius ratios were comparable to chromium(III) [34]. It has been found that the bidentate 3-hydroxypiridine-2-carboxylic acid (or Hhpic), whose molecule is similar to 1,2-HOPO-6-carboxylic acid, forms a copper(III) complex with a marked insulin-mimetic property [40]; however, there have been no reports on such the therapeutic property of metal complexes formed by either 1,2-HOPO or its derivatives, so far.

The previous computational study predicted the formation of two stable isomeric forms of the complex of chromium(III) with the ligand 1.2-HOPO-6-carboxylic acid: however there were no experimental evidences to prove such the theoretical prediction [41]. In the present work, the synthesis of the chromium(III) complex with the ligand 1,2-HOPO-6-carboxylic acid has been reported for the first time. A number of experimental methods have been applied in order to characterize the structures of the resulting complex. Computational methods have been found useful in gaining information on how the molecules of 1,2-HOPO-6-carboxylic acid chelate the chromium(III) ion as the insights into the chelation mechanism may lead to the development of novel metal complexes with improved structural and insulin-mimetic properties. Here the isomeric structures of the chromium(III) complex resulting from different pathways of chelation have been re-analyzed using the full molecular optimization under the density functional theory (DFT). The theory of computations used herein has been improved to the higher level at B3LYP/6-311++G(d,p) to ensure higher accuracy of the structural data as well as the molecular energetics of the complex. Computations of the infrared (IR) spectra have been performed based on the vibrational computations of the DFT-optimized isomeric structures. The UV/visible absorption spectra in water of the isomers have been generated according to the time-dependent DFT (TDDFT) computations with the polarizable continuum model (PCM) of solvation. Comparisons between the experimental and computational results allow more reliable justification on the most plausible chelation mechanism. In addition, with the aim at finding new anti-diabetic compound, the preliminary tests of insulin-mimetic effect have been carried out for the newly synthesized chromium(III) complex along with the other chromium-based compounds.

2. Experimental

2.1. General procedures

In the entire synthesis all chemicals used were of commercial reagent grade, and they were used without any further purification. The Fourier transform-infrared (FT-IR) spectra were recorded from KBr pellets containing the samples, using a Perkin–Elmer 2000 FT-IR Spectrometer. The ¹H NMR spectra were measured using a Bruker AVANCE 400 Ultrashield (400 MHz) Nuclear Magnetic Resonance Spectrometer. Measurement of the mass spectra of the samples was made using a Bruker MicroTOF Mass Spectrometer with electrospray ionization (ESI) operating in the negative ion mode.

2.2. Synthesis of the ligand 1,2-HOPO-6-carboxylic acid

The compound 1,2-HOPO-6-carboxylic acid was synthesized following the method developed by Xu [34] with minor modifications. As depicted in Scheme 1, this synthesis method consists of

two main successive steps. The detailed preparation route is described as follows. A solution of 6-hydroxy-picolinic acid was prepared by dissolving 5 g (0.036 mol) of 6-hydroxy-picolinic acid in a mixture of trifluoroacetic acid (30 mL) and glacial acetic acid (10 mL). A mixture of acetic anhydride (30 mL) and 30% H₂O₂ solution (10 mL) was prepared while cooling in an ice bath; this mixture was stirred for 4 h in order that a peracetic acid solution was formed. The 6-hydroxy-picolinic acid solution was added to this peracetic solution. The reaction mixture was then refluxed with stirring at 80 °C for 10 h, yielding a white precipitate. The excess trifluoroacetic acid was removed by vacuum distillation. The precipitate was filtered, washed with cold methanol and then dried. The product was a pinkish white solid of the compound 1,6-dihydroxy picolinic acid, yielding 4.63 g (82%); mp 209-210 °C. IR (KBr pellet): ν/cm⁻¹ 3440 (br, O—H stretch); 1734.7 (br. C=O stretch); 1211.1 (m, C-O stretch); 926.4 (br, O-H oop). H¹ NMR (DMSO- d_6): δ 7.42 (t. 1H. I = 8.8, 7.1 Hz): 6.64 (g. 2H. I = 7, 6.8 Hz); 3.43 (s, 1H, O—H). This compound was subsequently used as a precursor for the synthesis of 1,2-HOPO-6-carboxylic acid as follows. A solution of 1,6-dihydroxy picolinic acid was prepared by dissolving 4.63 g (0.029 mol) of 1,6-dihydroxy picolinic acid in 135 mL of 20% KOH(aq). This basic solution was refluxed at 70 °C for 12 h. The product was precipitated with 50 mL of cold concentrated HCl in an ice bath to keep the temperature below 20 °C throughout the process. A white precipitate was filtered and washed with 0.1 M HCl(aq), cold methanol and cold water successively. The product was dried under vacuum to yield 4.37 g (95%); mp 217–218 °C [42]. IR (KBr pellet): v/cm⁻¹ 3437.4 (br, O-H stretch); 1785.9 (br, C=O stretch); 1618.4 (m, C=O stretch); 929.7 (br, C—H deformation oop). H¹ NMR (DMSO- d_6): δ 7.43 (dd, 1H, J = 7, 9 Hz); 6.71 (dd, 1H, J = 1.6, 9 Hz); 6.64 (dd, 1H, I = 1.6, 7 Hz). MS (ESI-negative mode): m/z 154.01 (C₆H₄NO₄⁻).

2.3. Synthesis of the chromium(III) complex with 1,2-HOPO-6-carboxylic acid

Method A: A solution of chromium(III) was prepared by dissolving 0.54 g (2.03 mmol) of CrCl₂·6H₂O in 3 mL of deionized water. A suspension of ligand was made by dispersing 1.0 g (6.44 mmol) of 1,2-HOPO-6-carboxylic acid into 40 mL of deionized water with stirring. The solution of chromium(III) was then added to the suspension of ligand with stirring. The chromium-ligand mixture was refluxed with stirring at 80 °C under nitrogen atmosphere for about 24 h, allowing the formation of a green precipitate. This precipitate was separated from the reaction mixture by filtration and then washed with cold ethanol. After washing, the precipitate was re-crystallized in boiling chloroform. Chloroform was subsequently evaporated from the product solution at 40 °C using a rotary evaporator until the volume of solution was reduced to about 20 mL. The concentrated product solution had been left at room temperature for several days, allowing tiny crystals of the chromium(III) complex to be developed. These product crystals were filtered and dried in a vacuum oven. The crystal dimensions were, however, not sufficiently large for the single crystal X-ray diffraction measurement. The yield of product was 0.81 g (24.5%). Anal. Calcd. for C₁₈H₁₂N₃O₁₂Cr·H₂O: C 40.61; H 2.65; N 7.89. Found: C 39.20; H 2.89; N 7.59. IR (KBr pellet): v/cm⁻¹ 3439.3 (br, O—H stretch); 1753.6 (s, C=O stretch); 1616.1 (m, C=O stretch). MS (ESI-negative mode): m/z 512.98 ($C_{18}H_{11}N_3O_{12}Cr^-$). **Method B**: 1,2-HOPO-6-carboxylic acid (0.2329 g) was dissolved in 0.25 M $CH_3COOH(aq)$ (30 mL) with pH = 3.5, giving 0.05 M ligand solution. To prepare 0.05 M chromium(III) solution, CrCl₃·6H₂O (1.332 g) was dissolved in 0.25 M CH₃COOH(aq) (10 mL). Afterwards, the ligand solution was gently added to the chromium(III) solution without stirring. The resulting mixture was left at room temperature, allowing slow diffusion of the two components. After about

HO N COOH
$$\frac{\text{CH}_3\text{CO}_3\text{H, }80^\circ\text{C}}{\text{in CF}_3\text{COOH}}$$
 HO N COOH $\frac{(1)\ 20\%\ \text{KOH, }70^\circ\text{C}}{(2)\ 0.1\ \text{M HCI, } < 20^\circ\text{C}}$ O N COOH $\frac{\text{N}}{\text{OH}}$ COOH $\frac{\text{COOH}}{\text{OH}}$ 6-hydroxy picolinic acid 1,2-HOPO-6-carboxylic acid

Scheme 1. Synthesis method of 1,2-HOPO-6-carboxylic acid.

3 weeks the dark green crystals of the complex were produced. These crystals were slightly larger than those obtained by method A. The spectroscopic results for the complex prepared by method B also reproduced those for the complex prepared by method A.

3. Computational details

In the molecular designs of the complex, 1,2-HOPO-6-carboxylic acid was treated as a bidentate ligand using its two oxygen donor atoms upon chelation with chromium. Given the six-coordinate center of the complex, the metal-to-ligand mole ratio was 1:3. Nevertheless, as displayed in Fig. 1a, there are four positions of donor oxygen atoms which can possibly be responsible for the chelation with chromium. Theoretically, in order to maintain high molecular stability, two OH groups at positions 3 and 4 need to be located on the same side of molecule [41]. Assuming this theoretical configuration, it is unlikely for the ligand molecule to complete a chelate ring with metal ion by using the donor oxygen atom at position 4, as such the position is not only too distant from positions 1 and 2 but also too close to position 3. Thus it is fairly acceptable to consider only the oxygen atoms at positions 1, 2 and 3 for chelation; as a result, two isomeric structures of the complex designated as isomer 1 (Fig. 1b) and isomer 2 (Fig. 1c) can be formed. In the present study, the computational study on two isomeric structures of the complex of chromium(III) with the ligand 1,2-HOPO-6-carboxylic acid was attempted using the density functional theory (DFT). For each of the isomeric structures constructed, the gas-phase geometry optimizations and vibrational frequency calculations were carried out by the DFT method using the Gaussian 03 program [43]. The hybrid density functional B3LYP (i.e. Becke's three-parameter exchange functional [44] combined with the Lee-Yang-Parr correlation functional) [45] with the 6-311++G(d,p) basis set was applied to all DFT computations. The infrared (IR) spectral computations were carried out based

Fig. 1. (a) 1,2-HOPO-6-carboxylic acid in its doubly-protonated form. The oxygen atoms which can be donor atoms for metal chelation are at positions (1), (2), (3) or (4). Two isomeric structures of chromium(III) complex, designated as (b) isomer 1 and (c) isomer 2, can be formed through different pathways of chelation.

on the vibrational frequencies arising from the gas-phase DFT optimized structures, using the GaussSum 2.2.0 program [46]. In the IR spectral computations the Lorentzian peak shape was assumed, with the full width at half-maximum of 40 cm⁻¹. Five hundred data points were generated for each computed spectrum, with the wavenumber increment of 6 cm⁻¹. In order to estimate the absorption maxima for the UV/visible spectra in water, the TDDFT calculations at the B3LYP/6-311++G(d,p) level were carried out on each optimized structure, with the polarizable continuum model (PCM) accounting for the effects of hydration. Recently the TDDFT method has been claimed as being effective in describing the UV/visible absorption spectrum of the larger molecule of chromium(III) complex with six-coordinate metal center [47]. In the PCM approach, the optimized solute molecule was placed in the theoretical molecular cavity surrounded by a polarizable dielectric continuum of solvent (i.e. water, in this case, with the dielectric constant of 78.39). The cavity for solute molecule was built from a group of interlocking spheres, each of which was centered at the atomic position of non-hydrogen element in the solute molecule; the radii of these spheres were defined according to the UAKS United Atom Topological Model [48] implemented in the Gaussian 03 program. The GaussSum 2.2.0 program [46] was used to generate the UV/visible spectra, with the band shape defined by the Lorentzian function. Five hundred data points were generated for each UV/visible spectrum.

4. Results and discussion

4.1. ESI mass spectrometry

Fig. 2a and b shows the ESI mass spectra of the ligand 1,2-HOPO-6-carboxylic acid and its complex with chromium(III), respectively. Since the spectra were measured in the negative mode, the signals therefore arose from either molecular anions or anionic fragments of the compounds. In the spectra of both the ligand and its complex, the peak at m/z = 154 was ascribed to the formation of C₆H₄NO₄, the singly-deprotonated form of the ligand 1,2-HOPO-6-carboxylic acid (i.e. LH⁻ with the formula weight = 154) depicted as (a) in Scheme 2. Removal of carbon dioxide from LH⁻, as represented by (a) \rightarrow (b) in Scheme 2, produced the species $C_5H_4NO_2^-$ corresponding to the peak at m/z = 110 in the mass spectra of the ligand. In Fig. 2b, the most intense peak at m/z = 513 was due to the species $C_{18}H_{11}N_3O_{12}Cr^-$ with the formula weight = 513 [(d) in Scheme 2], formed by removing a single proton from a molecule of the complex $C_{18}H_{12}N_3O_{12}Cr$ [(c) in Scheme 2]. This result also implied the coordination of one chromium ion with three molecules of ligand. Furthermore as indicated by $(\mathbf{d}) \rightarrow (\mathbf{e}) \rightarrow (\mathbf{f}) \rightarrow (\mathbf{g})$ in Scheme 2, three successive steps of carbon dioxide removal from (d) generate the following species: (e) $C_{17}H_{11}N_3O_{10}Cr^-$, m/z = 469; (f) $C_{16}H_{11}N_3O_8Cr^-$, m/z = 425; **(g)** $C_{15}H_{11}N_3O_6Cr^-$, m/z = 381, all with the six-coordinate center remaining intact. It is worth considering that there would be low possibilities of three carbon dioxide molecules being eliminated from the coordination center if the carboxylate oxygen atoms were bound to the central metal ion. Regarding the relatively intense peak at m/z = 381 in the mass spectrum of

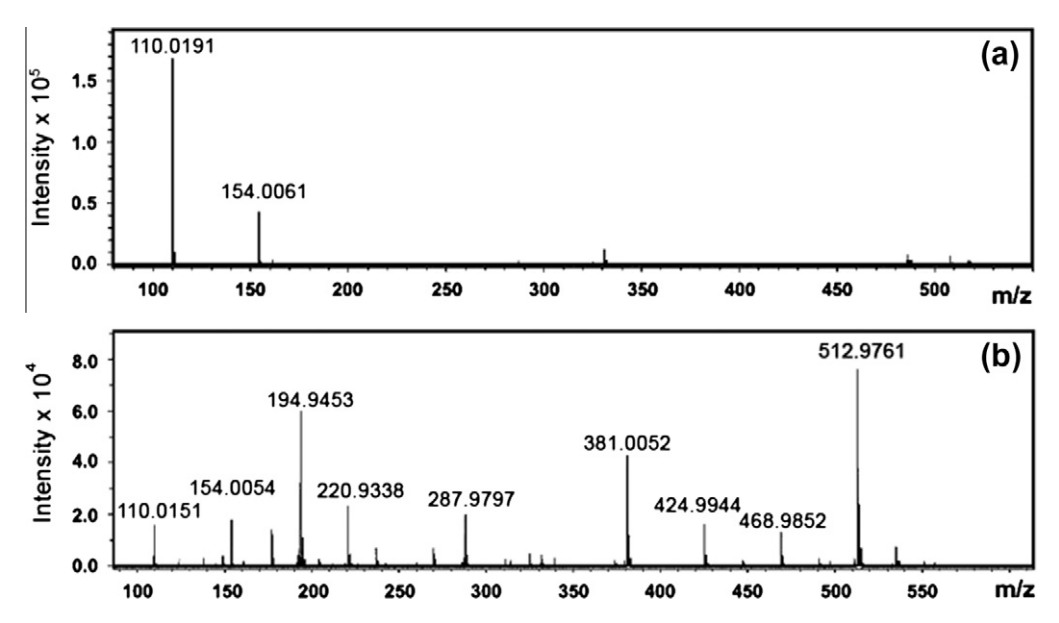


Fig. 2. ESI mass spectra measured in negative mode from (a) 1,2-HOPO-6-carboxylic acid and (b) the chromium(III) complex with 1,2-HOPO-6-carboxylic acid.

(a)
$$C_0 H_0 NO_4$$
 (b) $C_0 H_0 NO_2$ (c) $C_1 H_1 N_3 O_0 C C_1$ (d) $C_1 H_1 N_3 O_0 C C_1$ (e) $C_1 H_1 N_3 O_0 C C_1$ (f) $C_1 H_1 N_3 O_0 C C_1$ (g) $C_1 H_1 N_3 O_0 C C_1$ (f) $C_1 H_1 N_3 O_0 C C_1$ (g) $C_1 H_1 N_3 O_0 C C_1$ (f) $C_1 H_1 N_3 O_0 C C_1$ (g) $C_1 H_1 N_3 O_0 C C_1$ (f) $C_1 H_1 N_3 O_0 C C_1$ (g) $C_1 H_1 N_3 O_0 C C_1$ (f) $C_1 H_1 N_3 O_0 C C_1$ (g) $C_1 H_1 N_3 O_0 C C_1$ (f) $C_1 H_1 N_3 O_0 C C_1$ (g) $C_1 H_1 N_3 O_0 C C_1$

Scheme 2. Postulated forms of anionic species probed by ESI-mass spectrometry for either the chromium complex or the ligand.

the complex, the scenario that the carboxylate oxygen atoms participate in the metal chelation seems unlikely; therefore chelation of chromium by the pyridinone carbonyl oxygen atom

in the ligand would be more feasible. The other anionic species possibly formed upon molecular fragmentations of the complex are proposed in Scheme 2. The formula masses of the anionic

species shown in Scheme 2 agree well with the peak positions observed in the mass spectrum of the complex.

4.2. DFT optimized structures of the chromium(III) complex isomers

DFT/B3LYP/6-311++G(d,p)-optimized structures of the chromium(III) complex isomers were obtained as shown in Fig. 3. The geometries of both isomeric structures were successfully optimized by the DFT/B3LYP/6-311++G(d,p) approach. To be consistent with the mass spectroscopic data above, the metal-to-ligand mole ratio of 1:3 was adopted to the molecular design of both structures. Furthermore, in the formation of the complex it is fairly reasonable to limit the form of ligand to its singly-deprotonated form (LH⁻) since it has been shown previously by potentiometric method that with the relative populations up to 90% the LH- species of 1,2-HOPO-6-carboxylic acid in water dominates the other species $(LH_2 \text{ and } L^{2-})$ within a broad pH range of 2–7.5 [41], covering both the normal blood pH and the synthesis condition of the complex. Given the metal-to-ligand mole ratio of 1:3, the zero net charge on both isomeric structures was obtained. For each of the isomeric structures, deprotonation at the donor atoms bound to chromium was allowed to take place in order that electron-donating ability of these donor atoms was maintained at sufficiently high levels. As shown in Fig. 3 the chromium(III) ion is coordinated by either the carboxylate oxygen atoms (C-O-Cr) for isomer 1 or the pyridinone carbonyl oxygen atoms (C=O-Cr) for isomer 2. Both isomers, however, similarly use the oxygen atoms at the N-O groups to chelate chromium. The selected geometrical data for the DFT-optimized structures of the isomer 1 and isomer 2 of the complex are displayed in Table 1, where the atomic numbering for each isomer follows the graphic representation in Fig. 3. Three ligand molecules in each isomer show almost identical geometries. Both isomers with six-coordinate metal center similarly exhibit distorted octahedral geometries (see the relevant O-Cr-O bond angles in Table 1 for justification). The average Cr—O bond distances in both isomeric structures are similar at 1.99 Å, consistent with the crystallographic values for the same type of bond in the other chromium(III) complexes [49,50]. The distances between two oxygen atoms at two opposite vertices of the octahedral coordination are close to 3.96 Å for both isomers. The interatomic

distances H46-O34 in isomer 1 (1.88 Å) and H46-O34 in isomer 2 (1.66 Å) imply the slightly stronger intramolecular hydrogen bonding in isomer 2 than in isomer 1. Whereas the formation of six-membered chelate rings is noticeable in isomer 1, the isomer 2 structure contains five-membered chelate rings, each of which shows a high degree of planarity according to the dihedral angles Cr1-O39-C11-N30 (1.9°), O38-Cr1-O39-C11 (-2.9°) and O38-N30-C11-O39 (0.9°). Given the planar structure of an unbound ligand molecule, the dihedral angles C16-C14-C12-C11 (-0.1°) , C12—C11—N30—C18 (0.9°) , C14—C16—C18—N30 (0.1°) or H44-O36-C19-C18 (0.8°) in the isomer 2 structure suggest that, upon chelation each of the ligand molecules retain its planar structure, hence indicative of electron delocalization on the pyridinone ring. The dihedral angles Cr1-O38-N30-C11 (-3.3°), Cr1-O39-C11-N30 (1.9°) O38-N30-C18-C16 (179.1°) and 039—C11—C12—C14 (179.7°) in isomer 2 indicate that each chelate ring lies almost in the same plane as the pyridinone ring. On the other hand, the dihedral angle O36-C19-C18-N30 (-27.9°) in the isomer 1 structure suggests that while the donor atom O38 (at the N-O functional group) resides nearly in the same plane as the pyridinone ring (the dihedral angle $O38-N30-C11-C12 = -178.3^{\circ}$), rotation about the C19-C18 bond of the other donor atom O36 (the carboxylate oxygen atom) from the plane of pyridinone ring is necessary in the chelate ring formation. Because of the obvious distortion from planarity, the chelate rings in isomer 1 would be subjected to a strain that destabilizes them. According to the natural bond orbital (NBO) analysis, the principal donor-acceptor orbital interactions in isomer 1 are attributed to those between the lone-pair orbital (LP) on O34 and the unoccupied non-Lewis lone-pair orbital (LP*) on Cr1 with the interaction energy of 36.5 kcal mol⁻¹, and between the LP orbital on O33 and LP* orbital on Cr1 with the interaction energy of 28.6 kcal mol⁻¹. In the case of isomer 2 (the most stable isomer), the donor-acceptor orbital interactions: LP*(Cr1)-RY*(O34), LP*(Cr1)-RY*(O35), LP(O34)-LP*(Cr1) and LP(O35)-LP*(Cr1) are relatively strong, with the interaction energies of 45.2, 40.2, 35.1 and 40.2 kcal mol^{-1} , respectively (RY* denotes the non-Lewis Rydberg orbital). This suggests that the orbital interactions between the donor atoms and the metal ion in isomer 2 are stronger than those in isomer 1. The important

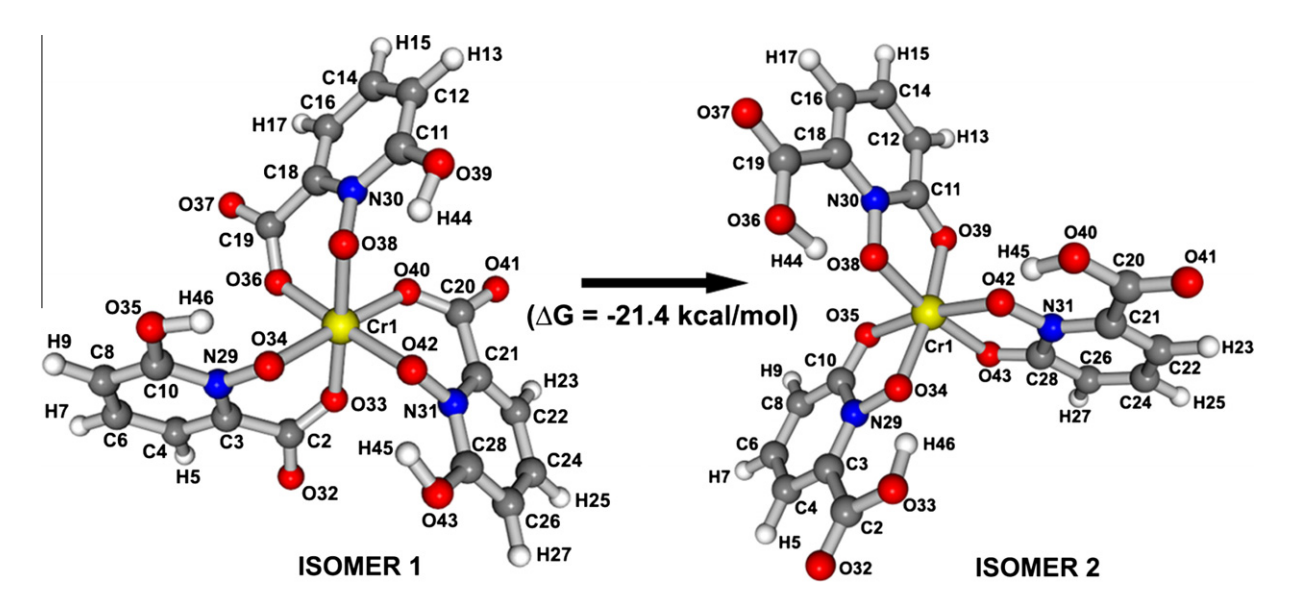


Fig. 3. Two isomeric structures for the chromium(III) complex with 1,2-HOPO-6-carboxylic acid as obtained from the DFT/B3LYP/6–311++G(d,p) optimization. Isomer 1 and isomer 2 denote the isomers with the higher and lower electronic energies, respectively. Some thermodynamic parameters (in kcal/mol) for the forward reaction noted here are as follows: $\Delta E = -19.9$, $\Delta G = -21.4$, and $\Delta H = -19.8$.

Table 1 Selected geometrical data for two isomers of the chromium(III) complex with 1,2-HOPO-6-carboxylic acid optimized by the DFT/B3LYP/6-311++G(d,p) approach.

	Isomer 1		Isomer 2	
Bond distance (Å)				
,	Cr1-033	1.95	Cr1-034	2.00
	Cr1-034	2.02	Cr1-035	1.98
	033-C2	1.29	034-N29	1.36
	O34-N29	1.35	O35-C10	1.28
	C10-035	1.32	033-C2	1.33
	C2-O32	1.22	C2-O32	1.20
	H46—034 ^a	1.88	H46-034 ^a	1.66
Bond angle (°)				
Coordination	O42-Cr1-O33	89.0	034Cr1038	92.6
	O33-Cr1-O36	94.8	034Cr1035	79.6
	033Cr1034	85.6	O38-Cr1-O42	92.7
	O38-Cr1-O40	89.0	039Cr1042	93.2
	O40Cr1O33	94.7	039Cr1043	95.2
	040—Cr1—042	85.6	043—Cr1—034	93.3
Chelate ring	033-C2-C3	117.3	C11-039-Cr1	115.5
	C2-C3-N29	121.1	Cr1-038-N30	112.5
	C3-N29-O34	122.9	N30-C11-039	117.2
	N29-034-Cr1	114.7	O38-N30-C11	115.1
Pyridinone ring	C3-C4-C6	120.3	C11-N30-C18	124.1
	C4-C6-C8	120.2	C14-C12-C11	120.1
	C6-C8-C10	118.6	C16-C14-C12	120.5
	C8-C10-N29	119.9	C18-C16-C14	120.0
	C10-N29-C3	122.7	N30-C18-C16	118.3
Dihedral angle (°)				
	O36-C19-C18-N30	-27.9	O38-N30-C18-C16	179.1
	O38-N30-C11-C12	-178.3	039-C11-C12-C14	179.7
	Cr1-033-C2-032	-175.0	Cr1-O38-N30-C11	-3.3
	C10-N29-O34-Cr1	131.0	Cr1-039-C11-N30	1.9
	C2-C3-N29-O34	-2.8	O38-N30-C11-O39	0.9
	C3-N29-O34-Cr1	50.1	038Cr1039C11	-2.9
	032-C2-C3-N29	152.3	C16-C14-C12-C11	-0.1
	032-C2-C3-C4	-28.2	037-C19-C18-C16	0.4
	N29-C3-C4-C6	1.4	C12-C11-N30-C18	0.9
	H5-C4-C6-H7	-0.8	H44-036-C19-C18	0.8
	C6-C8-C10-N29	0.3	H17-C16-C14-H15	0.2
	C6-C8-C10-O35	-179.3	C14-C16-C18-N30	0.1
	O35-C10-N29-C3	179.9	H13-C12-C11-039	-0.2

^a Intramolecular hydrogen bonds.

Table 2Important donor–acceptor orbital interactions as determined by the NBO analysis for two isomers of the chromium(III) complex with 1,2-HOPO-6-carboxylic acid.

Isomer	Orbital interactions		Energy (kcal mol ⁻¹)	
	Donor	Acceptor		
1	LP*(Cr1)	RY*(O34)	26.4	
	LP*(Cr1)	RY*(O33)	34.8	
	LP(O34)	LP*(Cr1)	36.5	
	LP(O33)	LP*(Cr1)	28.6	
2	LP*(Cr1)	RY*(O34)	45.2	
	LP*(Cr1)	RY*(O35)	40.2	
	LP(O34)	LP*(Cr1)	35.1	
	LP(O35)	LP*(Cr1)	40.2	

NBO donor–acceptor orbital interactions with their corresponding energies are also summarized in Table 2 for both isomers.

Evaluation of the total electronic energies and thermodynamic parameters for both structures, however, should be considered the most appropriate way to describe the molecular stability. According to the DFT/B3LYP/6–311++G(d,p) computations, the transformation in gas phase of isomer 1 into isomer 2 essentially reduced the total electronic energy (with the zero-point energy correction) by 19.9 kcal mol⁻¹, hence increasing molecular stability of the complex. With the negative Gibbs free energy

change of $-21.4 \, \rm kcal \, mol^{-1}$ and the negative enthalpy change of $-19.8 \, \rm kcal \, mol^{-1}$ at $298.15 \, \rm K$, such the transformation was exothermically spontaneous. The computational data here predicted that the formation of isomer 2 was more thermodynamically favorable than isomer 1, hence well supporting the hypothesis made from the ESI mass spectroscopic data in the previous section.

4.3. DFT computed-IR spectrum

Fig. 4a displays the IR spectrum measured from the complex of chromium(III) with the ligand 1,2-HOPO-6-carboxylic acid in solid phase. The spectra computed for the DFT-optimized isomers 2 and 1 of the corresponding complex are shown in Fig. 4b and c, respectively. No vibrational scaling factors were applied to the calculated IR frequencies. For both computed spectra, the distinguishable spectral details were found particularly in the frequency range of 1100–1900 cm⁻¹. Similar to the experimental spectrum in panel (a), the computed spectrum of isomer 2 in panel (b) featured a marked separation between two strong bands lying in the range of 1600–1900 cm⁻¹; however such the feature was missing in the computed spectrum of isomer 1. The vibrational computations revealed that the strong bands at 1813 and 1651 cm⁻¹ were assigned to the stretching modes of the C=O bonds in the carboxyl and pyridinone carbonyl groups of isomer

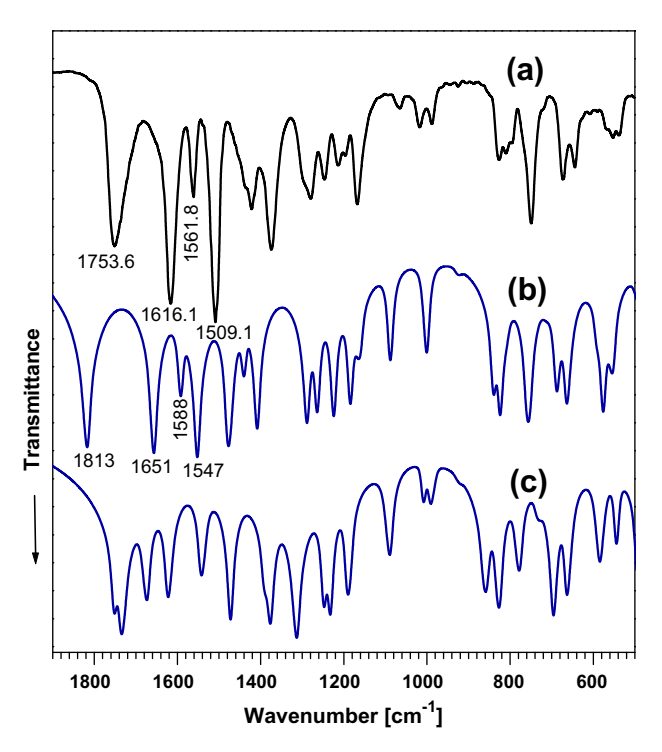


Fig. 4. (a) Experimental IR spectrum of the chromium(III) complex with 1,2-HOPO-6-carboxylic acid. The computed spectra of isomer 2 and isomer 1 for the corresponding complex are shown in (b and c), respectively.

2, respectively. In the experimental spectrum, such the two bands were found correspondingly at 1753.6 and 1616.1 cm⁻¹, lying in the lower frequency region than the computation. The separation between two C=O bands ($\approx 140 \text{ cm}^{-1}$) in the experiment was somehow narrower than that in the computation for isomer 2 $(\approx 160 \text{ cm}^{-1})$. Besides the C=O bands, the computation of the isomer 2 spectrum also predicted the presence of a medium band (1588 cm⁻¹) adjacent to a much stronger band (1547 cm⁻¹), both of which were ascribed to two modes of C.....C stretching in the pyridinone ring. As suggested by the vibrational computations, the stronger intensity of the lower-frequency band was due to the coupling with the C=O stretching in the pyridinone carbonyl group. The overall descriptions of two C......C stretching bands in the isomer 2 spectrum much resembled those of two experimental bands at 1561.8 and 1509.1 cm $^{-1}$. The differences in the vibrational frequencies between the experimental and computed spectra might arise from the fact that the IR spectrum was measured from the solid sample, whereas the computations were carried out based on the gas-phase molecular optimization. In solid phase such the intermolecular interaction as hydrogen bonding between the ligand molecules could considerably affect the spectrum. Nevertheless, the spectral computation as obtained for the isomer 2 structure (Fig. 4b) satisfactorily reproduced the descriptions of the experimental IR spectrum of the complex (Fig. 4a). Combined with the mass spectroscopic and computational results, this finding indicated that the isomer 2 structure of the complex was truly formed. Therefore, using the pyridinone carbonyl oxygen should be considered the most plausible pathway for the singly-deprotonated molecules of 1,2-HOPO-6-carboxylic acid to chelate the chromium(III) ion.

4.4. PCM/TDDFT-computed UV/visible spectra

In the UV/visible spectrum measured from the chromium(III) complex with 1,2-HOPO-6-carboxylic acid in water at pH = 3.5

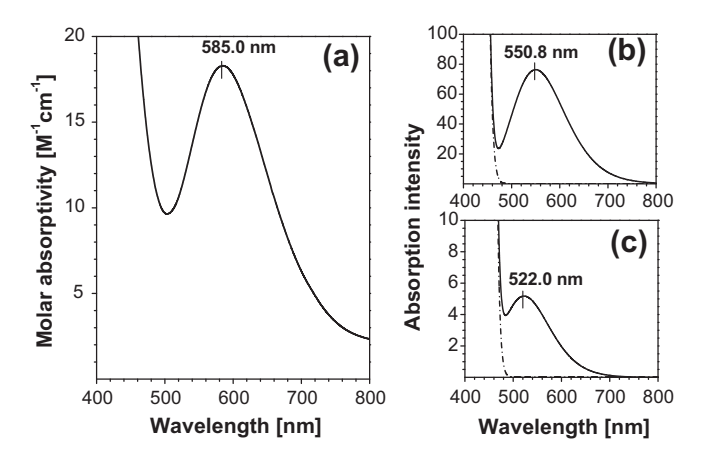


Fig. 5. (a) Experimental UV/visible spectrum in water of the chromium(III) complex with 1,2-HOPO-6-carboxylic acid. The computed spectra of isomer 2 and isomer 1 for the corresponding complex are shown in (b and c), respectively. The dashed lines indicate the spectral contribution of ligand.

(Fig. 5a), a characteristic absorption band of chromium(III) at 585.0 nm with the molar absorptivity of 18.3 M⁻¹ cm⁻¹ was observed. The strong absorption band of ligand dominated the spectrum most particularly in the UV region (at wavelengths shorter than 400 nm) as expected for the conjugated pyridinone derivative. Furthermore the dramatically large contribution of ligand absorption was not surprising regarding high molar proportion of ligand in the complex. The PCM(UAKS)-TDDFT/B3LYP/6-311++G(d,p) calculations predicted the maximum absorption at 522.0 nm for the UV/visible spectrum of isomer 1 in water (Fig. 5c), with relatively low oscillator strength (f) of 0.0001. Such the absorption was due to major contributions of the following orbital transitions: HOMO-1 → LUMO + 3 (15%) and HOMO → LUMO + 4 (11%), where "HOMO" and "LUMO" denote the highest occupied molecular orbital and the lowest unoccupied molecular orbital, respectively. In the spectrum of isomer 2 in water (Fig. 5b), the presence of an absorption band at the longer wavelength of 550.8 nm was predicted. This band was described by the computations as a convolution of three closely-lying absorption maxima at 570.6 nm [f = 0.0003, HOMO-1 \rightarrow LUMO + 4 (24%); HOMO \rightarrow LUMO + 3 (24%)], 545.3 nm [f = 0.0006, HOMO-3 \rightarrow LUMO + 4 (14%); HOMO-1 \rightarrow LUMO + 4 (21%); HOMO \rightarrow LUMO + 3 (21%)] and 545.0 nm [f = 0.0006, HOMO-3 \rightarrow LUMO + 3 (14%); HOMO-1 \rightarrow LUMO + 3 (21%); HOMO \rightarrow L + 4 (21%)]; a slight positive skewness of this band was due to the fact that the oscillator strength at the shorter wavelengths (545.0 and 545.3 nm) was twice larger than that at the longer wavelength (570.6 nm). Contrary to the isomer 1 spectrum, the separation between the ligand and the chromium absorption bands in the isomer 2 spectrum was well defined and this feature also resembled the experimental spectrum. Compared with the experiment, the theoretical predictions for isomer 1 and isomer 2 underestimated the wavelength of absorption maximum by 11% and 6%, respectively. In terms of both band positions and characteristics, the prediction for isomer 2 therefore matched the experiment better than that for isomer 1, and this finding supported the IR spectroscopic evidence. Following the PCM(UAKS)-TDDFT calculations, the transformation in water of isomer 1 into isomer 2 corresponded to the Gibbs free energy change in solution of -15.8 kcal/mol, indicating that such the transformation remained spontaneous under hydration. The Gibbs free energy change in solution was however lowered by 26% from the corresponding value in gas phase, reflecting significant effects of solvation on the isomerization.

4.5. Preliminary study on the insulin-mimetic effect of the complex

Diabetes in laboratory rats was induced by means of intraperitoneal injection (IP) of streptozotocin. The solution of chromium(III) complex with 1-hydroxy-2-pyridinone-6-carboxylic acid was injected to a group of diabetic rats whereas the other reference chromium(III) compounds, namely chromium(III) chloride and chromium(III) picolinate were used for the other groups. The diabetic rats in the control group received 0.9% normal saline. At different periods after injection, the blood samples were withdrawn from the rats and the glucose levels in plasma analyzed. It was found that injection of the chromium(III) complex with 1-hydroxy-2-pyridinone-6-carboxylic acid to diabetic rats was able to lower the plasma glucose levels by 40% in 5 h (see Supplementary Material for more information on this preliminary study).

5. Conclusions

The synthesis routes of the chromium(III) complex with the ligand 1,2-HOPO-6-carboxylic acid have been established. The mass spectroscopic evidence and elemental analysis suggested that the metal-to-ligand mole ratio of the complex was 1:3. Consistent with the theoretical prediction, the experimental spectroscopic data of the resulting complex indicated that the ligand 1,2-HOPO-6-carboxylic acid chelated the chromium(III) ion with its pyridinone carbonyl oxygen and N-oxide oxygen atoms. By this pathway of chelation, the ligand functioned as a bidentate chelating agent, forming the six-coordinate metal complex with the stabilized five-membered chelate rings. In addition, based on the preliminary results, the chromium complex synthesized for the present study exhibited promising insulin-mimetic property. To realize the therapeutic value of the complex, the response of blood glucose levels to oral administration as well as toxicity could be further investigated.

Acknowledgments

This research was financially supported by the Thailand Research Fund (Grant No. TRG478001) and the Faculty of Science, Burapha University, Thailand. The authors thank National Electronics and Computer Technology Center, Thailand for the computing resources and Assoc. Prof. Sirintorn Yibchok-anun for insulin-mimetic activity analysis.

Appendix A. Supplementary material

Supplementary data associated with this article can be found, in the online version, at http://dx.doi.org/10.1016/j.molstruc.2012. 07.041.

References

- [1] J.B. Vincent, Polyhedron 20 (2001) 1-26.
- [2] R.A. Anderson, J. Am. Coll. Nutr. 17 (1998) 548-555.
- [3] R.A. Anderson, Diabetes Metab. 26 (2000) 22-27.
- [4] H. Sakurai, Y. Kojima, Y. Yoshikawa, K. Kawabe, H. Yasui, Coord. Chem. Rev. 226 (2002) 187-198.
- [5] H. Watanabe, M. Nakai, K. Komazawa, H. Sakurai, J. Med. Chem. 37 (1994) 876-
- [6] H. Sakurai, Chem. Rec. 2 (2002) 237-248.
- [7] H. Sakurai, Y. Adachi, Biometals 18 (2005) 319-323.
- [8] Y. Adachi, J. Yoshida, Y. Kodera, A. Kato, Y. Yoshikawa, Y. Kojima, H. Sakurai, J. Biol. Inorg. Chem. 9 (2004) 885-893.

- [9] M. Yamaguchi, K. Wakasugi, R. Saito, Y. Adachi, Y. Yoshikawa, H. Sakurai, A. Katoh, J. Inorg. Biochem. 100 (2006) 260-269.
- Y. Yoshikawa, E. Ueda, H. Miyake, H. Sakurai, Y. Kojima, Biochem. Biophys. Res. Commun. 281 (2001) 1190-1193.
- Y. Yoshikawa, E. Ueda, K. Kawabe, H. Miyake, T. Takino, H. Sakurai, Y. Kojima, J. Biol. Inorg. Chem. 7 (2002) 68-73.
- C.M. Davis, J.B. Vincent, Biochemistry 36 (1997) 4382-4385.
- [13] H. Wang, A. Kruszewski, D.L. Brautigan, Biochemistry 44 (2005) 8167-8175.
- [14] G.W. Evans, U.S. Patent 4,315,927.
- 15] D.D.D. Hepburn, J.B. Vincent, J. Inorg. Biochem. 94 (2003) 86-93.
- [16] M.M. Bailey, J.G. Boohaker, R.D. Sawyer, J.E. Behling, J.F. Rasco, J.J. Jernigan, R.D. Hood, J.B. Vincent, Birth Defects Res. Part B 77 (2006) 244-249.
- [17] J.K. Speetjens, R.A. Collins, J.B. Vincent, S.A. Woski, Chem. Res. Toxicol. 12 (1999) 483-487. [18] X. Yang, S.Y. Li, F. Dong, J. Ren, N. Sreejayan, J. Inorg. Biochem. 100 (2006)
- 1187-1193.
- [19] P. Zhao, J. Wang, H. Ma, Y. Xiao, L. He, C. Tong, Z. Wang, Q. Zheng, E.K. Dolence, S. Nair, J. Ren, J. Li, Biochem. Pharmacol. 77 (2009) 1002-1010.
- [20] M.R. Kandadi, M.K. Unnikrishnan, A.K.S. Warrier, M. Du, J. Ren, N. Sreejayan, J. Inorg. Biochem. 105 (2011) 58-62.
- F. Dong, M.R. Kandadi, J. Ren, N. Sreejayan, J. Nutr. 138 (2008) 1846-1851.
- [22] Y. Adachi, J. Yoshida, Y. Kodera, A. Kato, Y. Yoshikawa, Y. Kojima, H. Sakurai, Biofactors 29 (2007) 213-223.
- G.R. Willsky, A.B. Goldfine, P.J. Kostyniak, J.H. McNeill, L.Q. Yang, H.R. Khan, D.C. Crans, J. Inorg. Biochem. 85 (2001) 33-42.
- [24] K.H. Thompson, J. Lichter, C. LeBel, M.C. Scaife, J.H. McNeill, C. Orvig, J. Inorg. Biochem. 103 (2009) 554-558.
- F. Li, X. Wu, T. Zhao, M. Zhang, J. Zhao, G. Mao, L. Yang, J. Trace Elem. Med. Biol. 25 (2011) 218-224.
- [26] D. Margina, B. Velescu, V. Uivarosi, V. Aldea, S. Negres, N. Mitrea, Febs J. 277 (2010) 61.
- [27] M. Badea, R. Olar, D. Marinescu, V. Uivarosi, V. Aldea, T.O. Nicolescu, J. Therm. Anal. Calorim. 99 (2010) 823-827.
- [28] J. Xu, D.G. Churchill, M. Botta, K.N. Raymond, Inorg. Chem. 43 (2004) 5492-
- [29] W.C. Floyd, P.J. Klemm, D.E. Smiles, A.C. Kohlgruber, V.C. Pierre, J.L. Mynar, J.M.J. Fréchet, K.N. Raymond, J. Am. Chem. Soc. 133 (2011) 2390-2393.
- [30] A. Datta, K.N. Raymond, Acc. Chem. Res. 42 (2009) 938-947
- [31] J.-M. Meyer, D. Hohnadel, F. Hallé, J. Gen. Microbiol. 135 (1989) 1479-1487.
- [32] H. Weizman, A. Shanzer, Chem. Commun. (2000) 2013-2014.
- [33] L.C. Uhlir, P.W. Durbin, N. Jeung, K.N. Raymond, J. Med. Chem. 36 (1993) 504-
- [34] J. Xu, P.W. Durbin, B. Kullgren, S.N. Ebbe, L.C. Uhlir, K.N. Raymond, J. Med. Chem. 45 (2002) 3963-3971.
- F. Paquet, V. Chazel, P. Houpert, R. Guilmette, B. Muggenburg, Radiat. Prot. Dosim. 105 (2003) 521-525.
- [36] P.W. Durbin, B. Kullgren, I. Xu, K.N. Raymond, Int. I. Radiat, Biol. 76 (2000) 199-214.
- [37] E.G. Moore, A. D'Aléo, J. Xu, K.N. Raymond, Aust. J. Chem. 62 (2009) 1300-1307
- [38] M. Seitz, K. Do, A.J. Ingram, E.G. Moore, G. Muller, K.N. Raymond, Inorg. Chem. 48 (2009) 8469-8479.
- [39] A. D'Alé o, E.G. Moore, G. Szigethy, J. Xu, K.N. Raymond, Inorg. Chem. 48 (2009) 9316-9324.
- [40] M. Nakai, F. Sekiguchi, M. Obata, C. Ohtsuki, Y. Adachi, H. Sakurai, C. Orvig, D. Rehder, S. Yano, J. Inorg. Biochem. 99 (2005) 1275–1282. K. Thipyapong, V. Ruangpornvisuti, J. Mol. Struct. 891 (2008) 1–10.
- [42] K.N. Raymond, R.C. Scarrow, D.L. White, U.S. Patent 4,698,431.
- [43] M.J. Frisch, G.W. Trucks, H.B. Schlegel, G.E. Scuseria, M.A. Robb, J.R. Cheeseman, J.A. Montgomery, T. Vreven, K.N. Kudin, J.C. Burant, J.M. Millam, S.S. Iyengar, J. Tomasi, V. Barone, B. Mennucci, M. Cossi, G. Scalmani, N. Rega, G.A. Petersson, H. Nakatsuji, M. Hada, M. Ehara, K. Toyota, R. Fukuda, J. Hasegawa, M. Ishida, T. Nakajima, Y. Honda, O. Kitao, H. Nakai, M. Klene, X. Li, J.E. Knox, H.P. Hratchian, J.B. Cross, V. Bakken, C. Adamo, J. Jaramillo, R. Gomperts, R.E. Stratmann, O. Yazyev, A.J. Austin, R. Cammi, C. Pomelli, J.W. Ochterski, P.Y. Ayala, K. Morokuma, G.A. Voth, P. Salvador, J.J. Dannenberg, V.G. Zakrzewski, S. Dapprich, A.D. Daniels, M.C. Strain, O. Farkas, D.K. Malick, A.D. Rabuck, K. Raghavachari, J.B. Foresman, J.V. Ortiz, Q. Cui, A.G. Baboul, S. Clifford, J. Cioslowski, B.B. Stefanov, G. Liu, A. Liashenko, P. Piskorz, I. Komaromi, R.L. Martin, D.J. Fox, T. Keith, M.A. Al-Laham, C.Y. Peng, A. Nanayakkara, M. Challacombe, P.M.W. Gill, B. Johnson, W. Chen, M.W. Wong, C. Gonzalez, J.A. Pople, Gaussian 03, Revision C.02, Gaussian Inc., Wallingford, CT, 2004.
- [44] A.D. Becke, J. Chem. Phys. 98 (1993) 5648–5652.
- [45] C. Lee, W. Yang, R.G. Parr, Phys. Rev. B 37 (1988) 785-789.
- [46] N.M. O'Boyle, A.L. Tenderholt, K.M. Langner, J. Comput. Chem. 29 (2008) 839-845
- [47] Y.-P. Tong, Inorg. Chim. Acta 362 (2009) 2167-2171.
- [48] V. Barone, M. Cossi, J. Tomasi, J. Chem. Phys. 107 (1997) 3210-3221.
- [49] D.M. Stearns, W.H. Armstrong, Inorg. Chem. 31 (1992) 5178-5184.
- [50] W. Fürst, P. Gouzerh, Y. Jeannin, J. Coord. Chem. 8 (1979) 237-243.